The Sterol Methyltransferases SMT1, SMT2, and SMT3 Influence Arabidopsis Development through Nonbrassinosteroid Products[1][W][OA]

Francine Carland, Shozo Fujioka, and Timothy Nelson*

Department of Molecular, Cellular, and Developmental Biology, Yale University, New Haven, Connecticut 06520 (F.C., T.N.); and RIKEN Advanced Science Institute, Wako-shi, Saitama 351–0198, Japan (S.F.)

Plant sterols are structural components of cell membranes that provide rigidity, permeability, and regional identity to membranes. Sterols are also the precursors to the brassinosteroid signaling molecules. Evidence is accumulating that specific sterols have roles in pattern formation during development. COTYLEDON VASCULAR PATTERNING1 (CVP1) encodes C-24 STEROL METHYLTRANSFERASE2 (SMT2), one of three SMTs in Arabidopsis (*Arabidopsis thaliana*). SMT2 and SMT3, which also encodes a C-24 SMT, catalyze the reaction that distinguishes the synthesis of structural sterols from signaling brassinosteroid derivatives and are highly regulated. The deficiency of SMT2 in the *cvp1* mutant results in moderate developmental defects, including aberrant cotyledon vein patterning, serrated floral organs, and reduced stature, but plants are viable, suggesting that SMT3 activity can substitute for the loss of SMT2. To test the distinct developmental roles of SMT2 and SMT3, we identified a transcript null *smt3* mutant. Although *smt3* single mutants appear wild type, *cvp1 smt3* double mutants show enhanced defects relative to *cvp1* mutants, such as discontinuous cotyledon vein pattern, and produce novel phenotypes, including defective root growth, loss of apical dominance, sterility, and homeotic floral transformations. These phenotypes are correlated with major alterations in the profiles of specific sterols but without significant alterations to brassinosteroid profiles. The alterations to sterol profiles in *cvp1* mutants affect auxin response, demonstrated by weak auxin insensitivity, enhanced *axr1* auxin resistance, ectopically expressed DR5:β-glucuronidase in developing embryos, and defective response to auxin-inhibited PIN2-green fluorescent protein endocytosis. We discuss the developmental roles of sterols implied by these results.

Sterols are integral components of the cell membrane and serve to provide stability to the phospholipid bilayer. In addition to this structural role, in higher plants, animals, and insects, sterols are precursors of the steroid hormones. There are over 100 types of sterols identified in plant species, but the most abundant are sitosterol, stigmasterol, and campesterol (Guo et al., 1995; Hartmann, 1998). The diversity in plants is in marked contrast to the single sterol accumulated in fungi and animals, ergosterol and cholesterol, respectively (Benveniste, 2004). The balance of phytosterols with varied properties has been postulated to provide membrane integrity under the broad range of temperatures to which plants are exposed (Beck et al., 2007).

Sterols are isoprenoid derivatives with a four-ring steroid nucleus (Edwards and Ericsson, 1999). A distinguishing feature of cholesterol and the major phytosterols is the number of carbons at the carbon 24 (C-24) position (Benveniste, 1986). Phytosterols have one to two additional carbons due to alkylation events catalyzed by *S*-adenosyl-L-Met-dependent C-24 STEROL METHYLTRANSFERASEs (SMTs; Fig. 1). SMT1 catalyzes the initial step in sterol biosynthesis by a single methyl addition at C-24 (C_1 addition). SMT2 and SMT3 can each add a second methyl group (C_2 addition), thus completing an ethyl side chain addition on C-24 (Husselstein et al., 1996; Bouvier-Navé et al., 1997; Schaller et al., 1998; Nes et al., 1999). In plants, cycloartenol is the primary starting compound in sterol biosynthesis and is the substrate of SMT1, although there is some promiscuity in substrate specificity among the SMTs (Diener et al., 2000). Arabidopsis (*Arabidopsis thaliana*) SMT2 and SMT3 can promote both C_1 and C_2 additions in a yeast *ergosterol6* mutant blocked at SMT1 and SMT2, and SMT1 can perform both methyl additions in bacteria (Husselstein et al., 1996; Bouvier-Navé et al., 1997). Recently, a second sterol pathway was identified that utilizes lanosterol rather than cycloartenol in its initial step. This lanosterol pathway is a minor branch, estimated to contribute a small fraction (1.5%) of total sitosterol (Ohyama et al., 2009). Redundancy among enzymes and path-

[1] This work was supported by the National Science Foundation (grant nos. IOS–0718881 and IBN–0416731 to T.N.) and by the Ministry of Education, Culture, Sports, Science and Technology of Japan (Grant-in-Aid for Scientific Research B no. 19380069 to S.F.).

* Corresponding author; e-mail timothy.nelson@yale.edu.

The author responsible for distribution of materials integral to the findings presented in this article in accordance with the policy described in the Instructions for Authors (www.plantphysiol.org) is: Timothy Nelson (timothy.nelson@yale.edu).

[W] The online version of this article contains Web-only data.

[OA] Open Access articles can be viewed online without a subscription.

www.plantphysiol.org/cgi/doi/10.1104/pp.109.152587

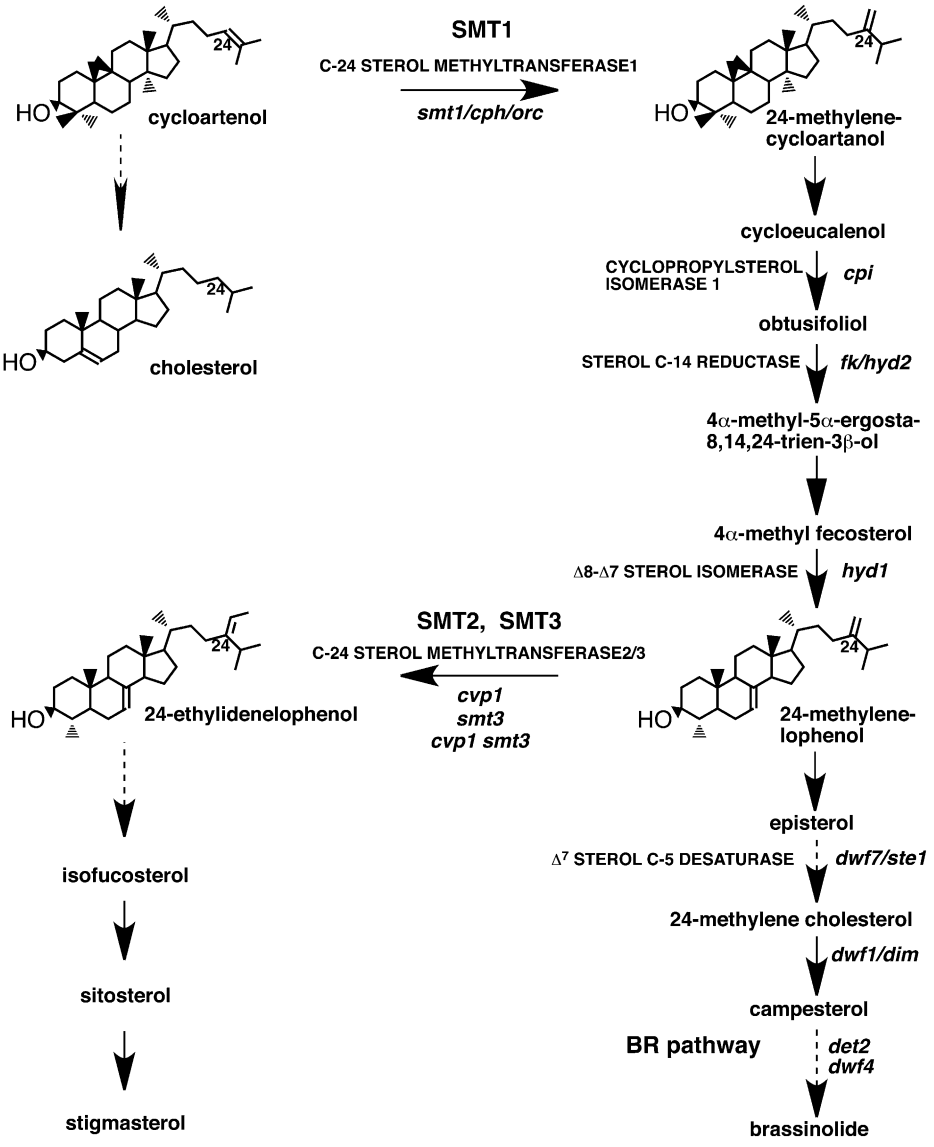

Figure 1. Phytosterol biosynthetic pathway. Key intermediates are shown. C-24, the site of SMT methyl additions, is indicated. Multiple steps are designated with dashed lines. Mutants are shown in italics with corresponding enzymes in uppercase letters. *dwf1/dim* has homology to FAD-linked oxidase and is predicted to have C-24 reductase activity.

ways ensures a balanced sterol composition and underscores the importance of sterols in plant growth and development.

Evidence is growing that specific sterols have regulatory roles in plants, independent of their contribution to brassinosteroid (BR) biosynthesis (Schaller, 2004). First, the phenotypes of sterol biosynthetic mutants are distinct from those in the downstream BR biosynthetic pathway. Mutants including *sterol methyltransferase1* (*smt1*; also called *cephalopod* [*cph*]), *fackel* (*fk*; allelic to *hydra2* [*hyd2*]), *hyd1*, *cyclopropylsterol isomerase* (*cpi*), and *cotyledon vascular pattern1* (*cvp1*) reveal roles for sterols in embryo, vein, shoot and root patterning, cell expansion, polarity and proliferation, fertility, cellulose level maintenance, gravitropism, and hormone signaling (Diener et al., 2000; Jang et al., 2000; Schrick et al., 2000, 2002, 2004a; Carland et al., 2002; Peng et al., 2002; Souter et al., 2002, 2004; Willemsen et al., 2003; Men et al., 2008). None of these are rescued by supplementation with BRs. In contrast, the dwarf phenotypes of BR biosynthetic mutants, including *dwarf7/sterol1* (*dwf7/ste1*) and *dwf1/dim*, are rescued by exogenous brassinolide (BL) application (Choe et al., 1999a, 1999b).

Second, transcriptional profiling experiments suggest that different sets of downstream genes are affected in sterol and BR pathway mutants. Microarray studies indicate some overlap between BR- and sterol-regulated cell expansion and division genes in the sterol mutant *fk* and the BR mutants *de-etiolated2* (*det2*) and *dwf4*, but overall the profiles are highly distinct, suggesting that independent targets are activated (Goda et al., 2002; He et al., 2003). Sterol mutants share characteristics and pathways with other hormones, providing additional evidence for sterols as hormonal regulatory molecules. Cholesterol, the major animal sterol, has a well-documented role as a transcriptional regulator through its modification of the

Hedgehog (Hh) ligand for the cell surface receptor Patched (Ptc; Incardona and Eaton, 2000). The Hh signal transduction pathway activates target genes in cell expansion and proliferation during embryonic and adult plant development (Duman-Scheel et al., 2002).

Third, sterol mutants influence membrane structure and traffic. The sterol biosynthetic mutants *smt1*^{orc}, *fk/hyd2*, *cpi*, and *cvp1* exhibit misdistribution of the polarly localized PIN protein, an efflux transporter of auxin, suggesting a sterol requirement at the level of PIN endocytosis (Simons and Ikonen, 1997; Souter et al., 2002; Willemsen et al., 2003; Men et al., 2008; Pan et al., 2009). In animals, cholesterol influences the polar trafficking of proteins through its ability to interact with sphingolipids in specialized membrane microdomains or lipid rafts (Simons and Ikonen, 1997). These membrane compartments serve to concentrate associated proteins for enhanced interaction and, thus, more efficient cellular processes. Likewise, sterol regulation in plants may not be solely at the transcriptional level.

Fourth, the sterol biosynthetic genes are expressed in regions of active cell division and expansion. Indeed, sitosterol, stigmasterol, and some abnormal *fk* sterols up-regulate characteristic cell expansion and proliferation genes (He et al., 2003). Sterol balance is affected in all mutants, but not always as predicted based on a simple linear pathway. For example, compromised SMT1 activity does not completely restrict further sterol transformations, as some downstream sterol levels remain unaffected (Diener et al., 2000). Consistent with this result, the *smt1* mutant phenotype, particularly at the adult stage, is relatively mild compared with other sterol biosynthetic mutants, even though *smt1* acts at the initial step. The downstream but more severe sterol mutants *fk*, *hyd1*, and *cpi* display a more drastic reduction in sterol levels, accumulate abnormal sterols, and show decreased BR precursor levels (Souter et al., 2002; Schrick et al., 2004a; Men et al., 2008). Furthermore, genetic data indicate a function for HYD1 and FK independent from SMT1 and suggest that the sterol biosynthetic pathway is more complex than previously believed (Schrick et al., 2002).

In this study, we provide further evidence that specific sterols influence numerous processes in plant development, independent of BR action. We previously reported on CVP1 as encoding SMT2, a branch point enzyme functioning to balance sterol and BR levels (Carland et al., 2002). Although SMT2 is expressed in regions of rapid cell division and cell expansion throughout development, the phenotypic abnormalities of *cvp1* mutants are predominantly restricted to a cotyledon vein pattern defect and do not share the gross embryo defects of *smt1*, *cpi*, *fk*, and *hyd1*. The close relative, SMT3, has a similar expression profile. Since overexpression of SMT3 can complement *cvp1* mutants, we reasoned that the mild *cvp1* phenotype may be due to genetic redundancy with *smt3*. Here, we assign function in plant development to the third SMT and report causal effects of depleting C-24 ethylidene SMTs both at the phenotypic and sterol levels. Our results reveal some novel roles for sterols, particularly in flower development. A complete BR profile shows that BR levels are unaffected in the *cvp1* mutant alleles, indicating that the phenotypic abnormalities are BR independent.

RESULTS

Identification of the *smt3* Mutant

SMT2 and SMT3 genes are highly homologous (83% identity) and encode highly similar sterol 24-carbon methyltransferases (Diener et al., 2000; Carland et al., 2002). The overexpression of SMT3 complements the cotyledon venation pattern defects of *cvp1* (SMT2) mutants. In addition, antisense *smt3* plants did not display a phenotype. These results suggest that SMT3 and SMT2 are functionally redundant. To investigate the effects of complete deficiency in C-24 ethylidene SMTs, we identified a T-DNA insertion in the coding region of SMT3 from the SALK SIGNAL collection (Fig. 2A) and combined it with the *cvp1* mutant allele of SMT2. The Arabidopsis SMTs are members of the methyltransferase superfamily, with the signature methyltransferase domain and an *S*-adenosyl-L-Met-binding region. *S*-Adenosyl-L-Met provides the methyl group for transfer to the

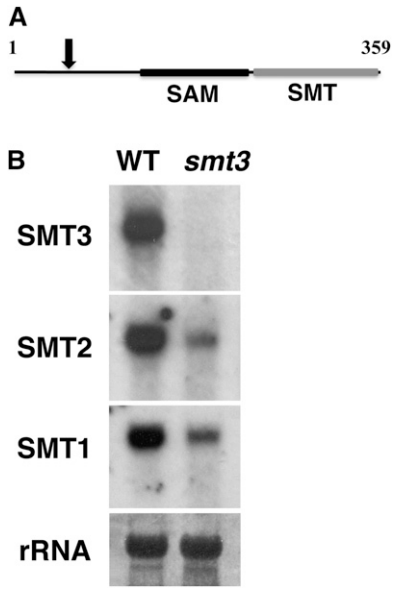

Figure 2. Identification of an *smt3* mutant. A, Predicted structure of the SMT3 protein. The arrow denotes the T-DNA insertion in SALK SIGNAL line 085292. Functional regions of the protein are indicated. SAM denotes the *S*-adenosyl-L-Met-binding sites. The SMT C-terminal domain is found in fungal and plant SMTs. B, RNA gel-blot analysis of SMT transcript levels in the *smt3* mutant. RNA was extracted from 7-d-old seedlings. The filter was probed sequentially after complete probe removal between hybridizations. WT, Wild type.

SMT substrate, 24-methylenelophenol (24-ML). The T-DNA insertion resides at amino acid 55 and is predicted to eliminate expression of the 359-amino acid SMT3 protein. RNA gel-blot analyses showed the absence of an SMT3 transcript in *smt3* mutants (Fig. 2B). As has been demonstrated previously with *cvp1* and *smt1* mutants, SMT1 and SMT2 transcript levels were reduced in the *smt3* mutant, suggesting that SMT transcription may be regulated through a sterol feedback mechanism (Diener et al., 2000; Carland et al., 2002).

SMT3 Is Functionally Redundant with SMT2

Although SMT3 transcripts are absent and SMT1 and SMT2 RNA levels are reduced in *smt3* mutants, *smt3* mutant seedlings are indistinguishable from the wild type (Fig. 3A). This result is consistent with the absence of an antisense plant phenotype and with genetic redundancy. *cvp1* seedlings have round, cupped epinastic cotyledons. *cvp1 smt3* double mutants are smaller and show enhanced epinasty with rounded, curved cotyledons (Fig. 3A; Table I). In comparison with wild-type cotyledon vein patterns, which consist of three to four continuous, closed loops, *cvp1* mutant cotyledons have a fragmented and less reticulated vein pattern (Table I; Carland et al., 1999). *cvp1* vascular cells are misshapen and exhibit abnormal planes of division that form knots of misaligned vascular cells (Fig. 3, B–D; Carland et al., 1999). Although *smt3* cotyledon vein patterns are identical to that of the wild type, the patterns of *cvp1 smt3* double mutants are less reticulated than either single mutant parent, with numerous misaligned vascular cells (Fig. 3, E–G; Table I). Defective SMT1 activity, which blocks sterol biosynthesis at an earlier step, results in similar vascular pattern defects (Fig. 3H; Willemsen et al., 2003). When a construct containing an SMT3 genomic clone was introduced into *cvp1 smt3* double mutants, it restored the less severe *cvp1* phenotype, indicating that the enhanced phenotypes observed in the *cvp1 smt3* double mutant were due to a dosage deficiency in SMT2 and SMT3 function (Fig. 3I). The rosette leaf vein patterns in the *cvp1* mutant resembled those of the wild type and of *smt3* mutants (Fig. 3J). However, the apical loop of the *cvp1 smt3* rosette consisted of poorly axialized cells and often freely terminated to form an open areole (area bordered by veins). At later stages, slow-growing *cvp1 smt3* double mutant plants displayed reduced stature and a loss of apical dominance, resulting in a bushy appearance (Fig. 3K), similar to cosuppressed SMT2 lines (Schaeffer et al., 2001). *cvp1 smt3* double mutants have short siliques and poor seed yield, reflecting either gametophytic or early embryo lethality (Fig. 3L; Supplemental Table S1). These results suggest that SMT3 is functionally redundant with SMT2 and that a complete deficiency in C-24 ethylidene SMT activity enhances the phenotypic abnormalities of *cvp1* by causing more absolute changes in the composition of sterol products.

Mutants Deficient in Both SMT1 and SMT2 Are Embryo Lethal

To investigate the effect of combined SMT1 and SMT2 deficiency, affecting two distinct steps in the sterol pathway, we attempted to generate a *cvp1 smt1* double mutant utilizing *smt1-1*-linked hygromycin resistance (HYG^R) as a selectable marker (Diener et al., 2000). Although we were able to construct a *cvp1* homozygous, *smt1* heterozygous (*cvp1/cvp1 SMT1/smt1;*HYG^R) plant, all self-fertilized HYG^R progeny (n = 101) were confirmed as the same genotype, suggesting that *cvp1 smt1* double mutants were embryo lethal (expect 19 *cvp1 smt1* double mutants). *cvp1/cvp1 SMT1/smt1* plants were identical to *cvp1* plants, with the exception of reduced silique length and an increase in aborted embryos (Supplemental Table S1; data not shown). This result confirms the sensitivity of embryo development to the balance of sterol species.

cvp1 smt3 Flowers Exhibit Morphological and Cellular Defects More Severe Than Those in Single Mutants

cvp1 is allelic to *frill1* (*frl1*), which was identified by its sepal and petal tip serrations (Hase et al., 2000, 2005). In *cvp1* mutants, serrations are restricted to the apical surface. *cvp1 smt3* double mutants have enhanced sepal and petal margin projections with highly abnormal cell expansion and division patterns that extend beyond the tips to lateral positions of the organs (Fig. 4, A–C). Enlarged nuclei were observed by 6-diamidino-2-phenylindole (DAPI) staining of *frl1* petal and sepal tip cells and were found to correlate with ectopic endoreduplication (Hase et al., 2005). Unlike wild-type petals and sepals, which had nuclei of uniform size, shape, and distribution, *cvp1 smt3* petal and sepal lobes displayed nonuniform, large, and often elongated nuclei (Fig. 4, D and E). This result is consistent with the reported cell expansion defects in other sterol mutants and supports the hypothesis that sterol composition influences cell division and expansion.

Flowers of *cvp1 smt3* double mutants display organ-spacing defects and homeotic organ transformations. Unlike wild-type, *cvp1*, and *smt3* flowers, in which floral organs are uniformly spaced within four concentric whorls, *cvp1 smt3* petals are improperly spaced, with overlapping petals and subsequent gaps (Supplemental Fig. S1). Late-forming flowers display unfused leaf-like carpels, increased carpel number, and homeotic transformations in which additional floral organs arise from fourth whorl gynoecia and deeply lobed leaf-like structures have stigma-like tips (Fig. 5). Floral defects are specific to *cvp1 smt3* flowers and do not appear in *smt1* (Supplemental Fig. S1). These results suggest that the alteration in sterol biosynthesis caused by SMT2 and SMT3 deficiencies has a significant impact on the proper growth of flowers.

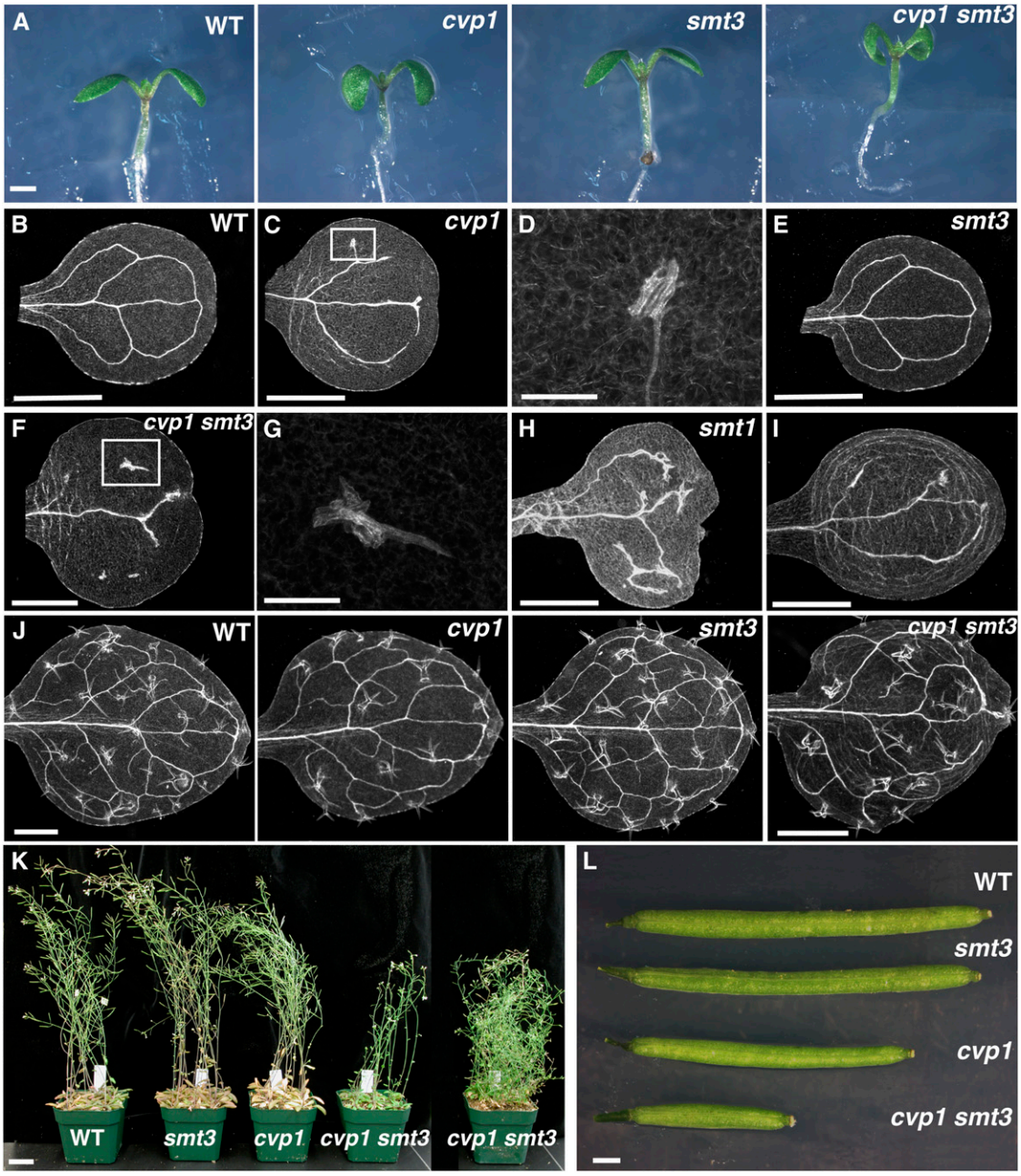

Figure 3. Developmental defects displayed in *cvp1 smt3* double mutants. A, Seven-day-old seedlings. *cvp1 smt3* double mutants show enhanced epinasty. B to I, Cotyledon vein patterns of cleared specimens viewed under dark-field optics. D, Higher magnification of the boxed region in C. F, *cvp1 smt3* double mutants have reduced vein length. G, Higher magnification of the boxed vascular island in F. H, *smt1-1* to show similar vein pattern defects among *smt* mutants. I, *cvp1 smt3* with genomic clone of SMT3 to show complementation of the *cvp1 smt3* double mutant cotyledon vein pattern. J, First rosette leaf vein patterns. K, Adult plant phenotypes. The first four pots are 6-week-old plants. *cvp1* plants are slightly dwarf. *cvp1 smt3* plants show retarded growth and reduced plant height. The 3-month-old *cvp1 smt3* plant on the far right shows excessive branching, resulting in a bushy appearance. L, Representative siliques to show reduced length in *cvp1 smt3* double mutants. Bars = 500 μm (A–C, E, and H–J), 50 μm (D and G), 250 μm (F), 3 cm (K), and 1 μm (L). WT, Wild type.

Root Defects in *cvp1 smt3* Double Mutants Resemble Those in *smt1*

SMT2 is expressed in internal cells throughout the developing embryo and has significant overlap with SMT3 expression in both early and late stages of root growth. Although *cvp1* and *smt3* mutant roots are indistinguishable from those of the wild type, many sterol biosynthetic mutants, including *smt1*, have se-

Table I. *Cotyledon vein patterns*

Values shown are means ± SD.

Genotype and Sample Size	Length	Width	Length of Lateral Veins[a]	Ratio[b]	No. of Vascular Islands[c]	Percentage with No Closed Areoles[d]
		mm				
Wild type (*n* = 34)	1.0 ± 0.11	0.9 ± 0.10	2.7 ± 0.57	2.7	0	0
cvp1 (*n* = 41)	1.0 ± 0.13	1.0 ± 0.13	1.65 ± 0.47	1.7	1.7 ± 1.2	82
smt3 (*n* = 30)	1.0 ± 0.09	0.9 ± 0.07	2.6 ± 0.36	2.6	0	0
cvp1 smt3 (*n* = 39)	0.68 ± 0.16	0.72 ± 0.19	0.58 ± 0.2	0.85	2.2 ± 1.8	97

[a]Values represent the sum of the lengths of all lateral veins. [b]Values represent the ratio of length of lateral veins to length of cotyledon. [c]Vascular islands are short stretches of isolated veins. [d]Area bordered by veins.

verely affected roots (Diener et al., 2000; Willemsen et al., 2003; Schrick et al., 2004a). Interestingly, *cvp1 smt3* double mutant roots displayed the severely affected roots of *smt1* mutants. *cvp1 smt3* roots were much shorter than those of the wild type or either single parent but were similar to *smt1* roots (Fig. 6A). Scanning electron microscopy of *smt1* and *cvp1 smt3* mutant epidermal cells showed a complete loss of aligned longitudinal cell files and abnormal cell expansion and morphology (Fig. 6B). These results suggest that critical sterols for proper root development are downstream from SMT2 and SMT3.

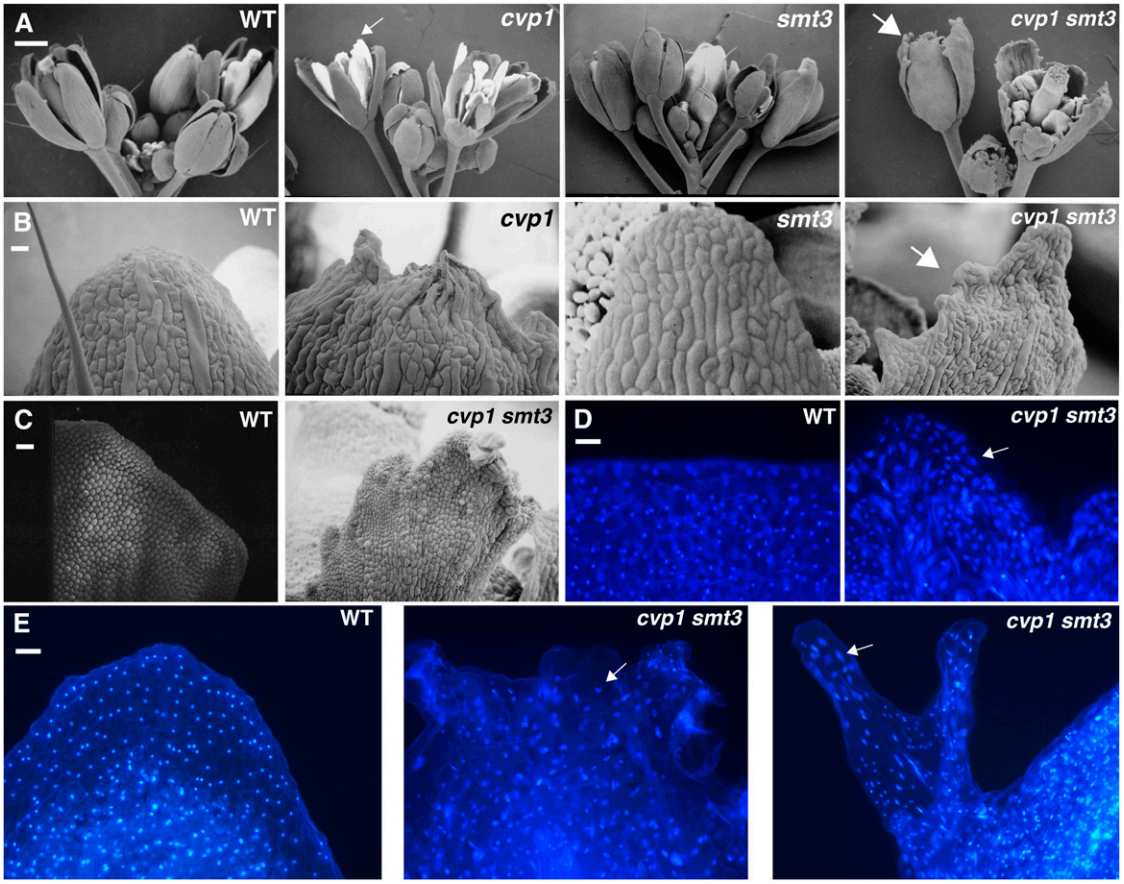

Figure 4. Enhanced sepal and petal tip serrations in *cvp1 smt3* double mutants correlate with enlarged nuclei. A to C, Scanning electron micrographs of inflorescences (A), sepal tips (B), and petal tips (C). *cvp1 smt3* inflorescences produce fewer flowers (A), have projections on tips and sides of sepals and petals (arrows, A–C), and display abnormal cell expansion on petal tips (C). D and E, DAPI staining of petals (D) and sepals (E) viewed under fluorescence to show enlarged and elongated nuclei in *cvp1 smt3* double mutants, indicated with arrows. E, Pronounced *cvp1 smt3* sepal projection. Bars = 750 μm (A), 500 μm (B and C), 100 μm, (D), and 50 μm (E). WT, Wild type.

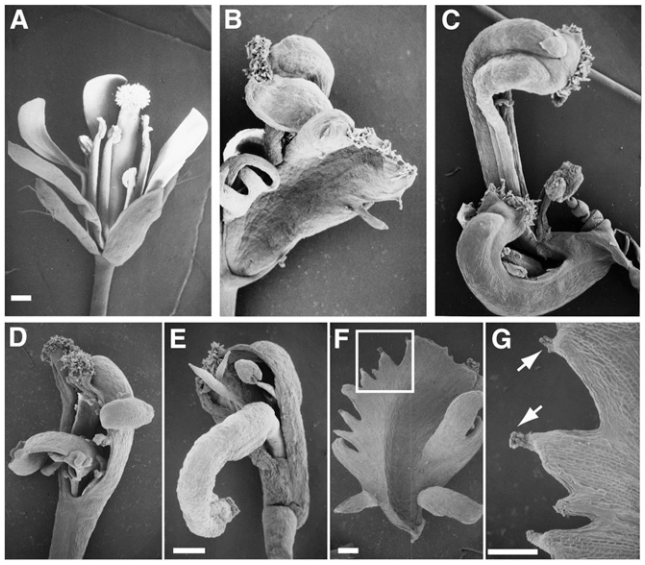

Figure 5. *cvp1 smt3* displays abnormal floral structures. Scanning electron micrographs show late-forming flowers in *cvp1 smt3* double mutants. A, Wild-type flower with sepals in outermost first whorl, petals in second whorl, stamens in third whorl, and a single gynoecium in the innermost fourth whorl. B to G, *cvp1 smt3* flowers. B and C, Multiple, unfused gynoecia. D and E, Fifth whorl reproductive organs emerging from gynoecia. F and G, Leaf-like structure with papillae. The boxed region of the leaf-like structure (F) is at a higher magnification (G) to show stigma-like surface (arrows). Bars = 500 μm.

Mutation in Both SMT2 and SMT3 Causes Extreme Alteration in Sterol Composition

SMT2 and SMT3 catalyze the second methyl addition onto the sterol compound 24-ML (Schaller et al., 1998; Benveniste, 2004). We compared the sterol profiles of *cvp1 smt3* seedlings with those of the wild type and *cvp1* and *smt3* single mutants (Table II). Consistent with its wild-type appearance, sterol levels were unaffected in the *smt3* mutant. Levels of sterol intermediates upstream of 24-ML were not affected in *cvp1* or *cvp1 smt3* mutants. However, as predicted, 24-ML was at increased amounts relative to that of the wild type and *smt3*. As a consequence of SMT2/3 deficiency, the quantity of the immediate product of SMT2 catalysis is reduced, particularly in the *cvp1 smt3* double mutant, in which 24-ethylidenelophenol is barely detectable. Levels of downstream sitosterol and campesterol branch products are also decreased in the *cvp1* single and *cvp1 smt3* double mutants. The end products of the sitosterol branch pathway, sitosterol, stigmasterol, and sitostanol, are dramatically reduced in the *cvp1 smt3* double mutant to only 1% to 3% of wild-type levels. Surprisingly, isofucosterol is relatively unchanged in *cvp1* but is greatly reduced in *cvp1 smt3*. Cholesterol lacks methyl additions; thus, it bypasses SMT activities and is elevated in *cvp1* single and *cvp1 smt3* double mutants.

The *cvp1 smt3* double mutant and the *smt1* single mutant exhibit similar abnormalities in root growth, fertility, and seedling morphology (Supplemental Fig. S2). Therefore, we compared the sterol composition in *cvp1 smt3* and in *smt1* to identify common features. SMT1 catalyzes the first methyl group addition using the substrate cycloartenol to initiate the sterol biosynthetic pathway. As reported previously for the *cph* allele of *smt1*, the cycloartenol content was strikingly increased in the *smt1* mutant allele. Similar to *cvp1 smt3* double mutants, sitosterol branch end products are in decreased quantities in *smt1*. The cholesterol branch of sterol biosynthesis is a minor branch, because intermediates feed into the dominant sitosterol and campesterol pathways. As previously reported with *smt1-1* and other *smt1* alleles, the amount of cholesterol is dramatically elevated, causing cholesterol to become the predominant sterol in *smt1* mutants. Although there are many similar trends between altered sterol content in *cvp1 smt3* and *smt1* mutants, the most noteworthy is the decrease in the major sterol, stigmasterol, raising the possibility that this sterol is essential for normal root growth and fertility. However, we cannot rule out the possibility that elevated

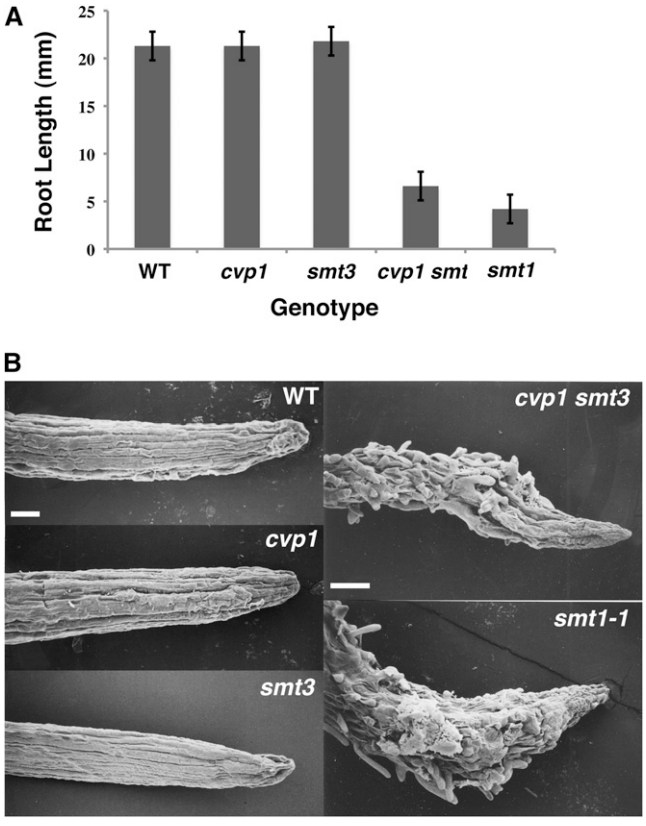

Figure 6. Similarities in root growth between *cvp1 smt3* double mutants and *smt1* mutants. A, Root length of 7-d-old seedlings. Values represent means of at least 75 samples from three biological replicates. Error bars represent SD. B, Scanning electron micrographs of 7-d-old medium-grown primary roots. Wild-type (WT), *cvp1*, and *smt3* roots show aligned longitudinal epidermal cell files. *smt1* and *cvp1 smt3* roots display abnormal epidermal cell patterns. Bars = 500 μm.

Table II. *Sterol profiles of smt mutants*

Values are given in $\mu g\ g^{-1}$ fresh weight. Sterol intermediates are listed in order of synthesis.

Sterol	Genotype				
	Wild Type	*cvp1-3*	*smt3*	*cvp1 smt3*	*smt1-1*
Upstream of SMT2/SMT3					
Cycloartenol	0.25	0.20	0.26	0.37	27
24-Methylenecycloartanol	0.49	0.34	0.53	0.40	0.04
Cycloeucalenol	0.18	0.14	0.19	0.09	0.06
Obtusifoliol	0.20	0.05	0.09	0.10	0.08
4α-Methyl-5α-ergosta-8,14, 24(28)-trien-3β-ol	0.02	0.01	0.02	0.02	0.01
24-ML (SMT2/SMT3 substrate)	0.09	1.2	0.07	1.5	0.14
Campesterol branch					
Episterol	0.03	0.23	0.04	0.67	0.27
24-Methlenecholesterol	0.69	7.0	0.77	16	21
Campesterol	20	67	22	99	26
Campestanol	0.29	0.97	0.29	2.04	0.49
6-Oxocampestanol	0.04	0.08	0.03	0.08	0.02
Brassicasterol	1.6	4.5	1.6	10	1.0
Sitosterol branch					
24-Ethylidenelophenol	0.38	0.08	0.41	0.01	0.06
Avenasterol	0.14	0.06	0.11	0.01	0.22
Isofucosterol	2.9	3.7	2.6	0.25	14
Sitosterol	120	61	113	3	34
Stigmasterol	9.4	8.0	5.5	0.10	0.67
Sitostanol	1.7	0.72	0.80	0.05	0.54
6-Oxositostanol	0.20	0.13	0.15	0.04	0.07
Cholesterol branch					
Cholesterol	1.6	7.3	5.5	11	31
Cholestanol	0.12	0.16	0.10	0.29	0.45
6-Oxocholestanol	0.03	0.04	0.02	0.05	0.06
Total sterol content	160	163	154	145	157

cholesterol also influences the observed developmental abnormalities. To test the ability of these sterols to rescue or mimic *smt* defects, we performed sterol supplementation experiments. Plants treated with stigmasterol and sitosterol were not able to restore *cvp1* cotyledon vein pattern or *cvp1 smt3* root defects to a wild-type phenotype (Supplemental Fig. S3, A and B), and cholesterol-supplemented wild-type seedlings did not mimic *smt* defects (Supplemental Fig. S3, B and C), suggesting that exogenously applied end product sterols are not sufficient to reestablish sterol balance, possibly due to insufficient uptake or metabolism.

BR Levels Are Unaffected in *cvp1* Alleles

The *cvp1* mutation results in an aberrant accumulation of the SMT2 substrate, 24-ML. This sterol intermediate feeds into the BR pathway to yield BL, the only known active steroid signaling molecule. With elevated precursor levels, it is possible that the *cvp1* mutant phenotype is due to alterations in the downstream BR levels. We previously showed that supplementation experiments of either wild-type plants with BL or *cvp1* plants with the BR inhibitor brassinazole (Brz) did not mimic or rescue the *cvp1* mutant phenotype, respectively, suggesting that alterations in the BR signaling molecules were not responsible for the phenotypic abnormalities (Carland et al., 2002). To assess whether BL levels are affected in *cvp1* mutant alleles, we performed BR profiling of *cvp1* 7-d-old seedlings. This allelic series has been described previously. Briefly, *cvp1-1*, *cvp1-3*, and *cvp1-4* are weak, null, and intermediate alleles, respectively (Carland et al., 2002). Sterol precursors to the BR pathway are elevated in all alleles, ranging from approximately 3- to 14-fold over wild-type levels, and are consistent with the severity of the alleles (Table III). The Arabidopsis BR biosynthetic pathway has two parallel pathways, one with early C-6 oxidation (i.e. 6-oxocampestanol, cathasterone) and the second with late C6 oxidation (i.e. 6-deoxocathasterone; Clouse and Sasse, 1998). These branches converge to produce the end product, BL. Although there were minor deviations in BR levels between the wild type and *cvp1* early in the pathway, there were no detectable differences in levels of biologically active BR. Low seed and tissue yield of *cvp1 smt3* double mutants precluded BR profiling. Therefore, to assess the effects of elevated BR precursor levels in *cvp1 smt3* double mutants, we performed supplementation experiments with the BL inhibitor, Brz (Sekimata et al., 2001). Exogenously applied Brz did not rescue *cvp1 smt3* developmental abnormalities (Supplemental Fig. S4). These results are consistent with our previous studies and indicate that the *cvp1*

Table III. *BR profiles of cvp1 alleles*
nd, Not detected.

Sterol	Genotype			
	Wild Type	*cvp1-1*	*cvp1-3*	*cvp1-4*
Sterol pathway (μg g^{-1} fresh weight)				
Episterol	0.029	0.29	0.30	0.20
24-Methylenecholesterol	0.46	4.34	6.47	5.03
Campesterol	12.9	48.1	63.3	47.5
Campestanol	0.18	0.74	1.25	0.64
6-Oxocampestanol	0.025	0.076	0.10	0.068
BR pathway (ng g^{-1} fresh weight)				
Late C_6 oxidation branch				
6-Deoxocathasterone	2.21	1.74	2.53	1.75
6-Deoxoteasterone	0.05	0.06	0.13	0.13
6-Deoxotyphasterol	0.36	0.40	0.59	0.48
6-Deoxocastasterone	1.41	1.82	1.16	1.69
Early C_6 oxidation branch				
Cathasterone	nd	nd	nd	nd
Teasterone	nd	nd	nd	nd
Typhasterol	0.03	0.02	0.03	0.02
Castasterone	0.11	0.12	0.11	0.10
BL	nd	nd	nd	nd

and *cvp1 smt3* mutant phenotypes are not associated with changes in BR levels and suggest that other sterols may act as signaling molecules.

cvp1 Enhances the Auxin Resistance of *axr1-3*

A number of the phenotypic abnormalities observed in *cvp1* and *cvp1 smt3* mutants are reminiscent of those in auxin signaling mutants. To investigate whether some of the phenotypic defects of *cvp1* are due to alterations in auxin signaling, we assayed the auxin sensitivity of *cvp1*. *cvp1* mutant seedlings exhibited weak auxin insensitivity relative to wild-type seedlings in root inhibition studies (Fig. 7A). Although there was no evidence of auxin resistance at higher levels of 2,4-dichlorophenoxy acetic acid (2,4-D) for the *cvp1* single mutant, the *cvp1 auxin resistance1-3* (*axr1-3*) double mutants show enhanced auxin resistance (Fig. 7B). This result is in agreement with the ability of *cvp1* to enhance auxin resistance of *transport inhibitor resistant1* (Pan et al., 2009).

Numerous auxin signaling mutants have a simplified vascular pattern, including *monopteros*, *axr1*, *axr6*, *bodenlos*, and *transport inhibitor resistant1*, indicating an involvement of auxin signaling in establishing the vein pattern (Przemeck et al., 1996; Hobbie et al., 2000; Deyholos et al., 2003; Hardtke et al., 2004; Carland and Nelson, 2009). To investigate the relationship between sterols and auxin in contributing to the complexity of the vein pattern, we examined the *cvp1 axr1-3* double mutant vein pattern. *axr1* mutant cotyledons have a reduced reticulum that usually consists of two loops with regions of poorly differentiated vascular cells indicated by nonuniform tracheary element thickening (Fig. 7C). Although the cotyledon vein pattern of *cvp1 axr1-3* was additive, sharing characteristics of both parents, the *cvp1 axr1-3* seedlings produced an enhanced *axr1-3* phenotype. Wild-type seedlings have an adaxially directed cotyledon cup. In *cvp1* and *cvp1 smt3* mutants, this cup is pronounced with raised cotyledon edges. In most cases (90%), *axr1* cotyledons are similar to those of the wild type, while the remaining 10% invert the concavity of the cup, resulting in an abaxially directed cup. Eighty-five percent of *cvp1 axr1-3* cotyledons have an abaxially oriented cup (Supplemental Fig. S5). Adult stages of plant growth are intermediate, indicating that the genetic relationship between *cvp1* and *axr1* is restricted to early stages of growth of specific organs (data not shown).

cvp1 Mutants Display Elevated Auxin Response

Although the cotyledon vascular pattern is established during embryogenesis, veins continue to develop throughout cotyledon expansion, as monitored with the vascular specific reporter gene Athb8::GUS (Baima et al., 2001; Kang and Dengler, 2002), and are possibly amenable to perturbation by the auxin transport inhibitor 1-*N*-naphthylphthalamic acid (NPA; Fig. 7D). Indeed, wild-type seeds germinated on NPA-supplemented medium displayed the nonuniform thickening characteristic of *cvp1*, indicating that compromised auxin transport results in a loss of vascular cell axialization (Fig. 7E). Similar to reports of NPA-treated leaves (Sieburth, 1999; Mattsson et al., 2003), NPA supplementation shifted and expanded regions of auxin accumulation in cotyledons, monitored with the synthetic auxin response reporter DR5::GUS (Fig. 7, F and G; Ulmasov et al., 1997). To examine auxin distribution in *cvp1* mutant developing embryos, we crossed plants containing the DR5::GUS reporter construct to *cvp1*. In developing wild-type embryos,

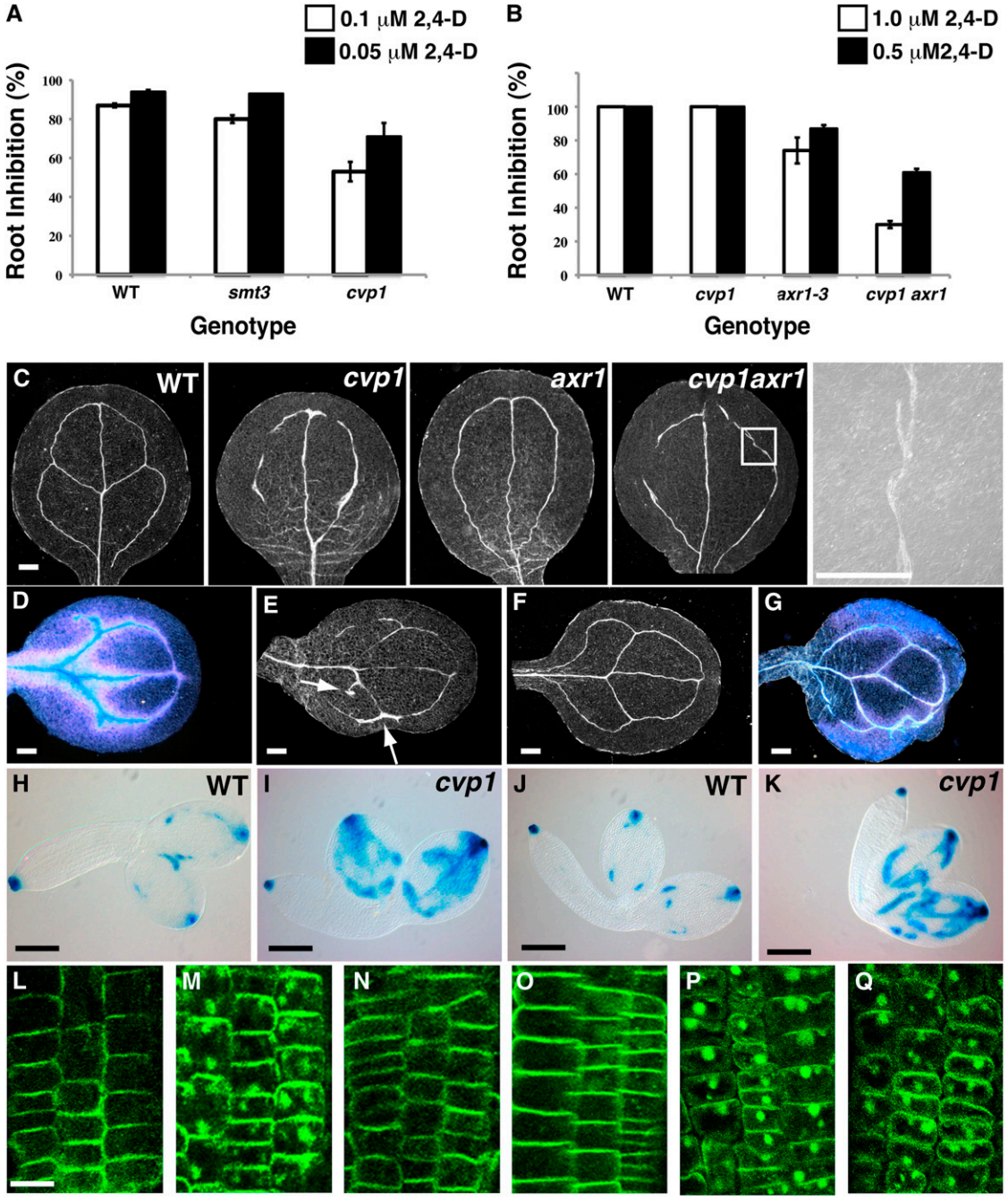

Figure 7. Auxin response of *cvp1* and *cvp1 smt3* mutants. A, *cvp1* mutants display weak auxin resistance. B, *cvp1* enhances auxin resistance of *axr1-3*. Root growth was measured 3 d after transfer of 4-d-old seedlings to MS medium or 2,4-D-containing MS medium. Root inhibition is the measurement of root growth on 2,4-D medium relative to that on medium without hormone expressed as a percentage. Values represent means of at least three experiments with measurements of approximately 40 seedlings per experiment. Error bars indicate SD. C, Cotyledon vein patterns to demonstrate the additive phenotype in *cvp1 axr1-3* double mutants. The image at the far right is the boxed region in *cvp1 axr1* at a higher magnification. D to G, Cotyledon vein patterns of wild-type medium-grown plants without NPA (D and F) and with NPA (E and G). D, Athb8::GUS expression viewed under dark-field optics to show that cotyledon veins are still developing and thus remain responsive to NPA-induced perturbations. Pink and blue staining is weak and strong GUS staining, respectively. E, NPA-induced cotyledon vein pattern defects (arrow). F, DR5::GUS-stained 2-week-old cotyledon. DR5::GUS expression is no longer visible at this stage. G, Enhanced DR5:GUS expression in margins of NPA-grown cotyledons. H to K, Representative DR5::GUS staining in developing embryos to show ectopic expression in *cvp1* mutants. H and I, Walking stick-stage embryos. J and K, Late bent cotyledon-stage embryos. L to Q, PIN2-GFP localization in wild-type (L–N) and *cvp1 smt3* (O–Q) roots in response to BFA (M and P) or NAA + BFA (N and Q). Bars = 100 μm (C and D–I), 200 μm (J and K), and 25 μm (L–Q). WT, Wild type.

DR5::GUS was visible in developing procambial strands and the hydathode of walking stick-stage embryos (Fig. 7H). At later stages, DR5::GUS staining was detectable in apical portions of basal loops in bent cotyledon-stage embryos, indicating its transient expression during vein initiation (Fig. 7J). In *cvp1* walking stick and bent cotyledon embryos, DR5::GUS was much stronger and broader, extending into areole portions beyond incipient vascular cells and the hydathode (Fig. 7, I and K). DR5::GUS root tip expression was indistinguishable between the wild type and *cvp1* and served as a control. This broad DR5::GUS expression correlated with the poorly axialized vascular cells of *cvp1* to reflect abnormalities in cotyledon vein patterns and is consistent with a *cvp1* defect in localized auxin transport.

Sterol Dependence of Auxin-Inhibited PIN2-GFP Endocytosis

PIN proteins facilitate auxin transport through trafficking between the plasma membrane and the internally localized endosome (Geldner et al., 2001). In the presence of brefeldin toxin A (BFA), PIN accumulates in endosomal aggregates known as BFA bodies. However, in response to auxin, BFA body formation is disrupted, because auxin promotes its own efflux by preventing internalization of PINs (Paciorek et al., 2005). To monitor auxin transport defects in the root, we crossed a PIN2-GFP line into *cvp1* and *cvp1 smt3* mutant backgrounds. Similar to results in wild-type roots, PIN2-GFP in *cvp1* and *cvp1 smt3* mutant roots is plasma membrane localized and responds appropriately to BFA with the formation of BFA bodies (Fig. 7, L and M; Supplemental Fig. S6, A and B). However, in contrast to wild-type roots, BFA bodies are retained in *cvp1* and *cvp1 smt3* mutants supplemented with auxin, demonstrating that correct sterol composition is required for auxin-inhibited PIN2-GFP endocytosis (Fig. 7, N and Q; Supplemental Fig. S6C).

DISCUSSION

Phenotypic Abnormalities Are Due to Altered Sterol Levels Independent of BR Signaling

The changes in the relative abundance of specific sterols caused by biosynthetic blocks have been associated with distinct developmental abnormalities. The SMT2 and SMT3 enzymes act at the branch point between sterol and BR synthesis. We show that in the *cvp1* and *smt3* mutants (in SMT2 and SMT3, respectively), the sterol content is dramatically affected without disrupting BR levels. This suggests that the vascular patterning defects observed in *cvp1* mutants are due to deficiency in particular sterols, rather than in BRs. Although other sterol mutants also have distinct patterning defects, suggesting that particular sterol imbalances have specific consequences, the extreme sterol block provided by the double *cvp1 smt3* mutant provides the most extensive detail thus far on the developmental processes affected by specific sterols.

Several mutants with sterol pathway blocks and consequent phenotypes have been characterized with regard to the specific sterols that accumulate. In wild-type plants, the sterol biosynthetic pathway produces a balance of key compounds, including the predominant end product sterol, sitosterol, the precursor to the BR pathway, campesterol, and the minor sterol, cholesterol. Mutations in upstream enzymes FK and HYD1 result in meristem and root patterning defects and are seedling lethal. In these mutants, overall typical sterol levels, including campesterol, decrease to 2% or less, with atypical sterols accounting for the majority of sterols (Schrick et al., 2004a). *smt* mutants show a more restricted phenotype, with a loss of polarity both at the vascular cell level and the organ level, characterized by rounded cotyledons, short roots, and reduced plant stature, and are able to grow to maturity, allowing an examination of sterol roles in adult development. Unlike *fk*, *hyd1*, and *cpi* mutants, total sterol levels in the *smt* mutants are approximately equivalent to wild-type levels, and there is no accumulation of abnormal sterols. Atypical sterols are not detected in *smt* mutants, most likely because the enzymes act at bifurcation steps and the accumulated substrate feeds into a parallel branch and is further transformed into sterol/steroid derivatives. Lastly, *smt* mutants are not depleted in BR precursor levels. Collectively, this argues that the less severe phenotype in *smt* mutants is due to reduced sitosterol levels and not to accumulated abnormal sterols or reduced BRs. However, it is also possible that elevated cholesterol or 24-ML has an impact on *smt* phenotypic abnormalities. The sterol profiles and phenotypes of *smt1* mutants are consistent with genetic evidence indicating distinct pathways between SMT1, FK, and HYD1 (Schrick et al., 2002).

Although the significant accumulation of cholesterol, which lacks methyl additions, in *smt* mutants is consistent with proposed SMT function, there were some inconsistencies with the relative amounts of downstream sterol products. Because SMT1 acts at the initial step in the pathway, it is predicted that all downstream products would be completely or significantly reduced, and although some sterol intermediates are reduced, some are at equivalent or increased levels relative to the wild type. For example, the downstream campesterol branch-specific sterol, 24-methylenecholesterol, is elevated in *smt1*. The presence of this methylated product may be due to promiscuity of SMT2 or SMT3 that is enhanced in SMT1-deficient plants. Likewise, even with complete deficiency of C-24 ethylidene SMT function, residual levels of downstream end product sitosterol are still detected in *cvp1 smt3* double mutants, albeit only at 2.5% of wild-type levels. These results suggest that alternative, not normally active, pathways are upregulated in sterol mutant backgrounds. Recently, it

was shown that the lanosterol pathway, the sterol biosynthetic pathway in yeast and animals, exists in plants (Ohyama et al., 2009). In wild-type plants, it is a minor pathway, contributing to only 1.5% of total sitosterol accumulation, but it could be exploited in *smt* mutant backgrounds and offers an explanation for the presence of downstream sterols.

Sterol Requirements for Cell Expansion and Cell Division

Sterols are abundantly synthesized during early stages of seed development, coincident with a period of intense cell division and membrane synthesis (Herchi et al., 2009). Some of the cell expansion and division defects in *fk*, *smt1*, *hyd1*, and *cvp1* may be the result of membrane structural defects from deficiency in specific sterols. Cell morphological defects in *fk*, *smt1*, and *hyd1* were shown to be associated with cell wall gaps and aberrant cell wall thickenings with ectopic deposits of lignin and callose (Schrick et al., 2004a). The sterol biosynthetic genes are expressed in regions of cell division and expansion, and SMT transcription is strongly induced by the cell division promoter, the cytokinins (Diener et al., 2000; Jang et al., 2000; Schrick et al., 2000; Carland et al., 2002; Souter et al., 2002). In addition, sterols are able to transcriptionally activate genes associated with cell expansion and proliferation (He et al., 2003). Lastly, specific sterol deficiencies are associated with defects in cellulose synthesis and deposition (Schrick et al., 2004a). The sterol mutants *smt1/cph*, *fk*, and *hyd1* exhibit a decrease specifically in bulk cellulose, without apparent effects on other cell wall components such as pectin and sugars. This result is consistent with the postulated role of the sterol conjugate, sitosterol-β-glucoside, as a primer of cellulose synthesis by providing Glc monomers to the developing cellodextrin chain (Peng et al., 2002). Although tight association of sitosterol-β-glucoside with cellulose was observed, recent evidence suggests that this interaction may not serve to prime biosynthesis. Mutations in the enzymes that catalyze the formation of sterol glucoside conjugates, UDP-Glc:sterol glucosyltransferase (i.e. *ugt80A2* and *ugt80B1* mutants), do not disrupt cellulose biosynthesis, nor does the single or double mutant combination display decreased cellulose levels relative to the wild type (DeBolt et al., 2009). Thus, if there is a sitosterol role in priming cellulose synthesis, there must be alternative enzymes, such as glucosylceramide synthase, which has the ability to produce glycosylated conjugates of sterols in vitro (Hillig et al., 2003). Alternatively, residual sterol glucosyltransferase in the *ugt80A2 ugt80B1* double mutants may be enough to facilitate the priming reaction.

The severe sterol block in the *cvp1 smt3* double mutant is associated with aberrant floral development. Although *fk* and *hyd1* mutants are seedling lethal, precluding an examination of sterol-dependent floral development, null *smt1* plants produce flowers and seeds. No floral defects are obvious in the *smt1-1* allele used in this study; however, *smt1*^{orc} displays ruffled sepals and mild gynoecia fusion similar to *cvp1* (Willemsen et al., 2003). *smt1*^{orc} is in the Utrecht background, and like other sterol mutants, it displays an ecotypic enhancement, suggesting that additional factors may be involved. Ectopic endoreduplication is associated with *cvp1* petal and sepal tip cell enlargement, suggesting that sterol-mediated cell cycle regulation may be responsible (Hase et al., 2005). Cholesterol-dependent cell cycle progression through Hh signal transduction has been reported (Incardona and Eaton, 2000). In this case, cholesterol covalently binds to the ligand, Hh. Modified Hh subsequently interacts with its partner, Ptc, and activates transcription of the primary regulators of the cell cycle to promote cell growth. If depleted of cholesterol, the cells were arrested in the G2 phase of mitosis but resumed phase progression with the addition of cholesterol or a cell cycle protein. In insects, a rough eye phenotype, consisting of enlarged eye cells due to abnormal cell expansion and strikingly reminiscent of *cvp1 smt3* petal cells, is a direct consequence of defective Hh signaling (Duman-Scheel et al., 2002). Therefore, it is conceivable that the cell expansion defects in the *smt* mutants may be due to a sterol ligand and its binding partner that acts in cell cycle regulation analogous to Hh/Ptc.

Mature ethylating SMT-depleted plants also induced misspecification of floral organ identity and closely resembled strong *ap2* mutants, characterized by a loss of petals and transformation of sepals to carpels (Bowman et al., 1991). AP2 and AP2-like transcription factors are regulated by microRNA172 (MiR172; Aukerman and Sakai, 2003). Overexpression of MiR172 induced stigmatic papillae on cauline leaf margins, closely resembling *cvp1 smt3* double mutant flowers. The means by which sterols influence floral patterning are unknown, but the observations suggest that sterols have roles in floral development and possibly share common pathways/targets with microRNA-regulated transcription factors. Another connection between sterols and microRNA-regulated gene expression is discussed below in relation to START domain proteins.

Sterols as Signaling Molecules

The phytosterol biosynthetic pathway leads to the production of the BRs, the only known steroid signaling molecules in plants (Belkhadir and Chory, 2006). Sterols themselves may act as signaling molecules in plants in a manner analogous to the action of cholesterol in mammalian systems. In these systems, the candidate target-binding partners for cholesterol are the steroidogenic acute regulatory protein-related lipid transfer (START) domain-containing proteins (Ponting and Aravind, 1999). These classic START domain proteins were reassigned as members of the helix-grip fold superfamily due to structural similarity in the ligand-binding pocket (Iyer et al., 2001). Mem-

bers of this superfamily have been demonstrated to bind a diverse range of molecules, including polyketide antibiotics, antigens, and RNA for both catalytic and noncatalytic activities. Plants contain numerous START domain proteins. One class of plant START protein receptors belonging to the helix-grip superfamily has been shown to bind the phytohormone abscisic acid via the START domain (Fujii et al., 2009; Ma et al., 2009; Melcher et al., 2009; Miyazono et al., 2009; Park et al., 2009; Santiago et al., 2009; Sheard and Zheng, 2009; Yin et al., 2009; Szostkiewicz et al., 2010). Other plant START domain proteins are homeodomain-Leu zipper (HD ZIP) transcription factors that serve to regulate plant morphogenesis, including meristem and vascular development, and thus are likely targets of sterol ligands (Schrick et al., 2004b). GLABROUS2 (GL2), a regulator of trichome and root hair development, acts to negatively regulate phospholipid signaling, thereby possibly integrating GL2 START domain ligand binding with downstream lipid signaling (Ohashi et al., 2003).

Of the approximately 90 HD transcription factor family members, 21 include START domains in an arrangement that only occurs in plants (Schrick et al., 2004b). This tight linkage may suggest a unique START domain transcriptional activation role in plants that relies on sterol ligands**.** Given the vein patterning defects in *smt* mutants, the vascularly expressed class III START domain HD ZIP subfamily (HD ZIP III) represents candidate SMT-mediated sterol targets (Prigge et al., 2005). However, these HD ZIP proteins, including PHABULOSA (PHB), PHAVOLUTA (PHV), REVOLUTA, Athb15/CORONA (CRN), and Athb8, are microRNA regulated within an evolutionally conserved site in the START domain, precluding an examination of sterol/START binding by mutational analysis (McConnell et al., 2001; Otsuga et al., 2001; Green et al., 2005; Kim et al., 2005; Melcher et al., 2009). Multiple loss-of-function mutant combinations reveal redundant, distinct, and antagonistic functions among HD ZIP III family members (Prigge et al., 2005). Interestingly, *phb phv cna* triple mutant flowers display reproductive organs within the fifth whorl, similar to *cvp1 smt3* mutant flowers. In addition, loss-of-function mutations in Athb-8 in a background of reduced MONOPTEROS function revealed a role for Athb-8 in vein patterning (Donner et al., 2009). Plant START domains are also coupled with other modules, including the phosphoinositide-binding pleckstrin homology domain, indicating a function for lipid control of intracellular signaling pathways (Schrick et al., 2004b). A specific function for phosphoinositide signaling in vein patterning involving CVP2 and its phosphoinositide target, the pleckstrin homology domain-containing VASCULAR NETWORK3/SCARFACE, was recently reported (Carland and Nelson, 2009). Collectively, these results support a possible role for sterol regulation of START domain proteins in influencing patterning events during plant morphogenesis.

Sterols, Membrane Domains, and PIN Proteins

Sterols are integral membrane components that serve not only a structural role but also a regulatory role by forming small membrane domains enriched in specific lipids that have an affinity for selected proteins (Incardona and Eaton, 2000). This confinement of selected proteins to specific small microdomains or rafts establishes a polarity to the cell. Although there is no direct evidence of the existence of microdomains in plants, due to technical difficulties in monitoring sterol distribution, there is circumstantial evidence accumulating with the identification of proteins from detergent-resistant membrane fractions (Boutte and Grebe, 2009). The PIN auxin efflux carrier family members have been proposed as likely candidates for sterol-enriched microdomain-localized proteins (Carland et al., 2002; Betts and Moore, 2003). Consistent with a function in directional transport of auxin, mutations that disrupt PIN activity or PIN asymmetric localization cause embryo, root, and vein polarity defects (Robert and Friml, 2009). Indeed, mislocalization of specific PIN family members has been shown in smt^{orc} and *hyd1* roots (Souter et al., 2002; Willemsen et al., 2003). In this report, we provide evidence that sterol-dependent endocytosis is required for efficient auxin transport. Both auxin signaling and correct sterol composition are required for auxin-inhibited endocytosis, as BFA bodies are retained in auxin signaling and sterol mutants, including *smt* mutants, in the presence of auxin (Pan et al., 2009).

The role of sterols in establishing cell polarity via PIN-mediated processes has been examined more closely with the characterization of *CPI*, which encodes the sterol biosynthetic enzyme CYCLOPROPYLESTEROL ISOMERASE1. *cpi* mutants are sterile, dwarf plants with small, compact rosettes and short roots and thus share characteristics with upstream *smt1* mutants and downstream *br* mutants (Men et al., 2008). CPI localized to the cell plate-associated endoplasmic reticulum and supports endoplasmic reticulum as a site of sterol synthesis, as biochemical studies have suggested. Newly synthesized sterols are subsequently transported to the plasma membrane via the Golgi apparatus (Grebe et al., 2003). Upon BFA treatment, plasma membrane sterols are internalized to early endosomes, colocalizing with PIN2. Similar to other sterol mutants, PIN2 was mislocalized in *cpi* mutants (Men et al., 2008). A detailed analysis indicated that PIN2 failed to redistribute asymmetrically at the end of cytokinesis in the endocytosis-defective *cpi* mutants, indicating a sterol dependence for establishing PIN asymmetry. Thus, the observed vein polarity defects in *smt* mutants may be a direct consequence of a disruption in sterol-mediated PIN endocytosis. Failure to transport auxin within veins is consistent with the ectopic DR5::GUS expression observed in *cvp1* and smt^{orc} mutants and with the *cvp1* enhanced auxin resistance of *axr1* and thus is likely responsible for the *smt* vein patterning defects. It will be interesting to

examine the sterol dependence of additional PIN family members, particularly PIN5, which has been shown to reside in the endoplasmic reticulum, the site of sterol biosynthesis (Mravec et al., 2009). In summary, studies with *cvp1* and additional sterol mutants indicate that sterols have multiple functions independent of BR signaling molecules. Future work will be to further elaborate on the mechanisms of SMT-derived sterols.

MATERIALS AND METHODS

Plant Material, Growth Conditions, Mutant Selection, and Treatments

All genotypes were in Arabidopsis (*Arabidopsis thaliana*) ecotype Columbia with the exception of *smt1-1* (kindly provided by Dr. Gerald Fink), which had been identified in an Ac-mutagenized Wassilewskija population. Therefore, we crossed *smt1-1* into the Columbia ecotype for at least five generations before use in this study, utilizing the tightly linked hygromycin antibiotic resistance marker to aid in selection. There were no differences in the *smt1* phenotype between Columbia and Wassilewskija backgrounds. The *cvp1-3* null allele was used throughout this study, except where noted otherwise. All seeds were surface sterilized prior to growth on Murashige and Skoog (MS) medium (MS salts [Sigma M0404], 1% Suc, and 0.75% agar, pH 5.7). Seven-day-old seedlings were used for analysis or transplanted to soil (1.5:1 Farfard premium fine soil:vermiculate) and grown under a 16-h-light cycle with 175 μmol m^{-2} s^{-1} illumination at 22°C with 50% relative humidity in environmental chambers. Under these more recent growth conditions, the *cvp1-3* allele is not as severe as was previously reported. The *smt3* allele is a SALK T-DNA insertion line (SALK_085292) and was obtained from the Arabidopsis Biological Resource Center (ABRC). Sequencing of amplified PCR products was used to verify the T-DNA insertion site (LBA1, 5′-GGTTCACG-TAGTGGGCCATCG-3′; SMT3-5, 5′-CGTTGCAGAGAGAATCAAGTCC-3′). Homozygous *smt3* mutants were selected by PCR using the primers SMT3-5 and SMT3-8 (5′-CACAAACCATTTTAGGTG-3′). *cvp1 smt3* double mutants were verified by sequence analysis and PCR for the *cvp1-3* (F14MT1, 5′-GGTCTTCCTCACTCTTAACG-3′; F14MT2, 5′-GCACCGTCGAAACTGT-TGTC-3′) and *smt3* alleles, respectively. Plants homozygous for *cvp1* and heterozygous for *smt1-1* were verified by hygromycin resistance and PCR (for presence of the Ac element, AD333, 5′-CGGTTATACGATAACGGTCG-3′ [Diener et al., 2000]; SMT1-1, 5′-CTCCGATTCATCTTTATCCTC-3′; to test for homozygous *smt1-1* line, SMT1-1 and SMT1-7, 5′-GGACCATCTCTCACTC-ATC-3′). *axr1-3* seeds were provided by the ABRC. To make the *cvp1 axr1-3* double mutant, 4-d-old F2 progeny were transferred to 0.1 μM 2,4-D-supplemented medium and grown vertically for 4 d. Auxin-resistant individuals were transferred to soil and monitored for the *cvp1* ruffled sepal and petal phenotype. These putative *cvp1 axr1-3* double mutants were verified by sequencing (AXR1-3F, 5′-GAGAATCCAGACACGTTG-3′; AXR1-3R, 5′-CGGCTCTGATACATT-CAG-3′). For NPA (Sigma) studies, seeds were germinated on medium supplemented with 20 μM BFA and grown for 2 weeks. For *cvp1 smt3* rescue experiments, medium was supplemented with the solvent (mock), 1 μM Brz (kindly provided by Tadao Asami), or 1 μM sitosterol and 1 μM stigmasterol (Sigma) dissolved in ethanol (10 mM stock). Higher concentrations of stigmasterol and sitosterol in the medium inhibited plant growth. For *cvp1* rescue experiments, plants were treated for the duration of embryo development with 50 μM sitosterol and 50 μM stigmasterol. Wild-type seeds were germinated and grown on 10 μM cholesterol-supplemented medium (Sigma; 10 mM stock in ethanol). Root inhibition on 2,4-D (Sigma) was performed as described (Carland and Nelson, 2009). Columbia seeds containing the DR5::GUS construct were provided by Dr. Andrew Cary with permission from Dr. Jane Murfett. Athb-8::GUS seeds were provided by Dr. Nancy Dengler. PIN2-GFP was donated by Dr. Gloria Muday with permission from Dr. Ben Scheres.

RNA Gel-Blot Analysis

Molecular biology techniques were derived from standard protocols. Total RNA was extracted from 7-d-old seedlings using the Trizol reagent (Invitrogen). RNA (10 μg per lane) was loaded for RNA gel-blot analysis. To ensure equal loading, ribosomal RNA was detected after overnight transfer to a nylon filter (Zetaprobe; Bio-Rad) using the methylene blue staining method (Herrin and Schmidt, 1988). Full-length SMT1, SMT2, and SMT3 cDNA probes were PCR amplified from constructs and labeled using the High Prime labeling kit (Roche). Primers used to generate probes have been reported and are as follows: for SMT1, SMT1-1 and 5′-GGGCATGTGCACATGATTCAG-3′; for SMT2, 5′-GGTCTTCCTCACTCTTAACG-3′ and 5′-GTCAGTAGTGTTA-CTCACACAGGC-3′; for SMT3, 5′-CAGAGTCGTGAACTTAACG-3′ and 5′-CCAATAGAATTTCCCGGC-3′. Hybridizations were performed overnight at 42°C in a formamide-based buffer and washed under stringent conditions (Carland et al., 2002). Filters were stripped of the probe by boiling in 0.1× SSC (15 mM sodium chloride, 1.5 mM trisodium citrate)/0.05% SDS between hybridizations.

Microscopy

Vein patterns were imaged as described previously (Carland et al., 2002). For quantitation of cotyledon size and vein patterns, cleared, mounted specimens from 7-d-old seedlings were captured using Axiovision software on a Zeiss Axiophot microscope and measured with ImageJ software. Plant images were captured on a Zeiss dissecting microscope using Axiovision software. Samples were prepared for scanning electron microscopy by fixation in ethanol:acetic acid (3:1) overnight at 4°C and dehydrated in an ethanol series to 100% ethanol. The remaining preparation and microscopy were performed as reported (Carland and McHale, 1996). For DAPI staining, flowers of similar developmental stages were cleared in 70% ethanol for 2 h at room temperature. Samples were subsequently incubated in 1 μM DAPI in 70% ethanol for 1 h, rinsed three times with 0.5× MS, mounted in 0.5× MS/10% glycerol, and viewed under fluorescence on a light compound microscope (Zeiss Axiophot). GUS staining of embryos has been described in a previous report (Carland and Nelson, 2004). For PIN2-GFP studies, roots of 9-d-old seedlings were treated with 50 μM BFA (Sigma) for 90 min or a 30-min pretreatment of 10 μM naphthalene-1-acetic acid (NAA; Sigma) followed by incubation with 10 μM NAA and 50 μM BFA for 90 min (Pan et al., 2009). PIN2-GFP imaging was conducted on a Zeiss LSM 510 Meta NLO confocal microscope (Carl Zeiss International).

Constructs and Plant Transformation

The SMT3 construct for complementation of the *cvp1 smt3* double mutant was generated by PCR amplification of the transcriptional unit (approximately 2.8 kb, containing a 1.5-kb promoter, an approximately 1-kb coding region, and a 0.3-kb 3′ untranslated region) of SMT3 from Columbia using the primers SMT3-2 (5′-CGTGTGAGCAAATAGATCACG-3′) and SMT3-9 (5′-CTAATTTCCAGTGATCCATC-3′). The amplified product was cloned into pCR2.1 TOPO vector (Invitrogen), sequenced to ensure that there were no base pair changes, and subsequently subcloned into pCAMBIA 2300 using compatible restriction sites. The construct was electroporated into *Agrobacterium tumefaciens* strain GV3101 and transformed into *smt3* plants using the floral dip method (Clough and Bent, 1998). Several transgenic plants were selected on medium with 50 μg mL^{-1} kanamycin and crossed to *cvp1-3* mutants. Kanamycin-resistant F1 progeny from independent transformants were self-pollinated, and the resulting kanamycin-resistant F2 progeny were scored for cotyledon vein pattern, root, and petal defects. There was no evidence of the *cvp1 smt3* double mutant phenotype among 401 kanamycin-resistant progeny. A portion of kanamycin-resistant *cvp1* plants were genotyped as *cvp1 smt3*.

Measurement of BR and Sterol Levels

One gram and 20 g of 7-d-old lyophilized seedling tissue were used for sterol and BR profiling, respectively. Purification and quantification of sterols and BRs were carried out as described previously (Fujioka et al., 2002; He et al., 2003).

Sequence data from this article can be found in the GenBank/EMBL data libraries under accession numbers NM_101884 (SMT2) and NM_106258 (SMT3).

Supplemental Data

The following materials are available in the online version of this article.

Supplemental Figure S1. *smt* mutant petal phenotypes.

Supplemental Figure S2. *cvp1 smt3* double mutants share characteristics with *smt1* mutants in fertility and seedling morphology.

Supplemental Figure S3. Sterol supplementation does not rescue or mimic *smt* defects.

Supplemental Figure S4. The BL inhibitor Brz does not rescue *cvp1 smt3*.

Supplemental Figure S5. *cvp1 axr1-3* double mutants show reversal of cotyledon concavity.

Supplemental Figure S6. Auxin inhibition of PIN2-GFP endocytosis requires correct sterol balance.

Supplemental Table S1. Silique length of *smt* mutants.

ACKNOWLEDGMENTS

We thank the ABRC, Dr. Jane Murfett, Dr. Andrew Cary, Dr. Nancy Dengler, Dr. Gerald Fink, Dr. Gloria Muday, and Dr. Ben Scheres for providing seeds, Barry Piekos for advice with scanning electron microscopy, Dr. Joseph Woelinski and Patrick Cournoyer for advice with confocal microscopy, Dr. Stephen Dellaporta for use of the lyophilizer, and Dr. Suguru Takasuto for supplying deuterium-labeled internal standards for sterol and BR analysis. We acknowledge Dr. Neeru Gandotra and Dr. S. Lori Tausta for comments on the manuscript.

Received December 23, 2009; accepted April 19, 2010; published April 23, 2010.

LITERATURE CITED

Aukerman MJ, Sakai H (2003) Regulation of flowering time and floral organ identity by a microRNA and its APETALA2-like target genes. Plant Cell **15:** 2730–2741

Baima S, Possenti M, Matteucci A, Wisman E, Altamura MM, Ruberti I, Morelli G (2001) The Arabidopsis ATHB-8 HD-zip protein acts as a differentiation-promoting transcription factor of the vascular meristems. Plant Physiol **126:** 643–655

Beck JG, Mathieu D, Loudet C, Buchoux S, Dufourc EJ (2007) Plant sterols in "rafts": a better way to regulate membrane thermal shocks. FASEB J **21:** 1714–1723

Belkhadir Y, Chory J (2006) Brassinosteroid signaling: a paradigm for steroid hormone signaling from the cell surface. Science **314:** 1410–1411

Benveniste P (1986) Sterol biosynthesis. Annu Rev Plant Physiol **37:** 275–308

Benveniste P (2004) Biosynthesis and accumulation of sterols. Annu Rev Plant Biol **55:** 429–457

Betts H, Moore I (2003) Plant cell polarity: the ins-and-outs of sterol transport. Curr Biol **13:** R781–R783

Boutte Y, Grebe M (2009) Cellular processes relying on sterol function in plants. Curr Opin Plant Biol **12:** 705–713

Bouvier-Navé P, Husselstein T, Desprez T, Benveniste P (1997) Identification of cDNAs encoding sterol methyl-transferases involved in the second methylation step of plant sterol biosynthesis. Eur J Biochem **246:** 518–529

Bowman JL, Smyth DR, Meyerowitz EM (1991) Genetic interactions among floral homeotic genes of Arabidopsis. Development **112:** 1–20

Carland F, Nelson T (2009) CVP2- and CVL1-mediated phosphoinositide signaling as a regulator of the ARF GAP SFC/VAN3 in establishment of foliar vein patterns. Plant J **59:** 895–907

Carland FM, Berg BL, FitzGerald JN, Jinamornphongs S, Nelson T, Keith B (1999) Genetic regulation of vascular tissue patterning in *Arabidopsis*. Plant Cell **11:** 2123–2137

Carland FM, Fujioka S, Takatsuto S, Yoshida S, Nelson T (2002) The identification of CVP1 reveals a role for sterols in vascular patterning. Plant Cell **14:** 2045–2058

Carland FM, McHale NA (1996) LOP1: a gene involved in auxin transport and vascular patterning in Arabidopsis. Development **122:** 1811–1819

Carland FM, Nelson T (2004) Cotyledon *vascular pattern2*-mediated inositol (1,4,5) triphosphate signal transduction is essential for closed venation patterns of *Arabidopsis* foliar organs. Plant Cell **16:** 1263–1275

Choe S, Dilkes BP, Gregory BD, Ross AS, Yuan H, Noguchi T, Fujioka S, Takatsuto S, Tanaka A, Yoshida S, et al (1999a) The Arabidopsis *dwarf1* mutant is defective in the conversion of 24-methylenecholesterol to campesterol in brassinosteroid biosynthesis. Plant Physiol **119:** 897–907

Choe S, Noguchi T, Fujioka S, Takatsuto S, Tissier CP, Gregory BD, Ross AS, Tanaka A, Yoshida S, Tax FE, et al (1999b) The *Arabidopsis dwf7/ste1* mutant is defective in the *delta7* sterol C-5 desaturation step leading to brassinosteroid biosynthesis. Plant Cell **11:** 207–221

Clough SJ, Bent AF (1998) Floral dip: a simplified method for Agrobacterium-mediated transformation of Arabidopsis thaliana. Plant J **16:** 735–743

Clouse SD, Sasse JM (1998) Brassinosteroids: essential regulators of plant growth and development. Annu Rev Plant Physiol Plant Mol Biol **49:** 427–451

DeBolt S, Scheible WR, Schrick K, Auer M, Beisson F, Bischoff V, Bouvier-Nave P, Carroll A, Hematy K, Li Y, et al (2009) Mutations in UDP-glucose:sterol glucosyltransferase in Arabidopsis cause transparent testa phenotype and suberization defect in seeds. Plant Physiol **151:** 78–87

Deyholos MK, Cavaness GF, Hall B, King E, Punwani J, Van Norman J, Sieburth LE (2003) VARICOSE, a WD-domain protein, is required for leaf blade development. Development **130:** 6577–6588

Diener AC, Li H, Zhou W, Whoriskey WJ, Nes WD, Fink GR (2000) Sterol methyltransferase 1 controls the level of cholesterol in plants. Plant Cell **12:** 853–870

Donner TJ, Sherr I, Scarpella E (2009) Regulation of preprocambial cell state acquisition by auxin signaling in Arabidopsis leaves. Development **136:** 3235–3246

Duman-Scheel M, Weng L, Xin S, Du W (2002) Hedgehog regulates cell growth and proliferation by inducing cyclin D and cyclin E. Nature **417:** 299–304

Edwards PA, Ericsson J (1999) Sterols and isoprenoids: signaling molecules derived from the cholesterol biosynthetic pathway. Annu Rev Biochem **68:** 157–185

Fujii H, Chinnusamy V, Rodrigues A, Rubio S, Antoni R, Park SY, Cutler SR, Sheen J, Rodriguez PL, Zhu JK (2009) In vitro reconstitution of an abscisic acid signalling pathway. Nature **462:** 660–664

Fujioka S, Takatsuto S, Yoshida S (2002) An early C-22 oxidation branch in the brassinosteroid biosynthetic pathway. Plant Physiol **130:** 930–939

Geldner N, Friml J, Stierhof YD, Jurgens G, Palme K (2001) Auxin transport inhibitors block PIN1 cycling and vesicle trafficking. Nature **413:** 425–428

Goda H, Shimada Y, Asami T, Fujioka S, Yoshida S (2002) Microarray analysis of brassinosteroid-regulated genes in Arabidopsis. Plant Physiol **130:** 1319–1334

Grebe M, Xu J, Mobius W, Ueda T, Nakano A, Geuze HJ, Rook MB, Scheres B (2003) Arabidopsis sterol endocytosis involves actin-mediated trafficking via ARA6-positive early endosomes. Curr Biol **13:** 1378–1387

Green KA, Prigge MJ, Katzman RB, Clark SE (2005) CORONA, a member of the class III homeodomain leucine zipper gene family in *Arabidopsis*, regulates stem cell specification and organogenesis. Plant Cell **17:** 691–704

Guo DA, Venkatramesh M, Nes WD (1995) Developmental regulation of sterol biosynthesis in Zea mays. Lipids **30:** 203–219

Hardtke CS, Ckurshumova W, Vidaurre DP, Singh SA, Stamatiou G, Tiwari SB, Hagen G, Guilfoyle TJ, Berleth T (2004) Overlapping and non-redundant functions of the Arabidopsis auxin response factors MONOPTEROS and NONPHOTOTROPIC HYPOCOTYL 4. Development **131:** 1089–1100

Hartmann MA (1998) Plant sterols and the membrane environment. Trends Plant Sci **3:** 170–175

Hase Y, Fujioka S, Yoshida S, Sun G, Umeda M, Tanaka A (2005) Ectopic endoreduplication caused by sterol alteration results in serrated petals in Arabidopsis. J Exp Bot **56:** 1263–1268

Hase Y, Tanaka A, Baba T, Watanabe H (2000) FRL1 is required for petal and sepal development in Arabidopsis. Plant J **24:** 21–32

He JX, Fujioka S, Li TC, Kang SG, Seto H, Takatsuto S, Yoshida S, Jang JC (2003) Sterols regulate development and gene expression in Arabidopsis. Plant Physiol **131:** 1258–1269

Herchi W, Harrabi S, Sebei K, Rochut S, Boukhchina S, Pepe C, Kallel H (2009) Phytosterols accumulation in the seeds of Linum usitatissimum L. Plant Physiol Biochem **47:** 880–885

Herrin DL, Schmidt GW (1988) Rapid, reversible staining of northern blots prior to hybridization. Biotechniques **6:** 196–197

Hillig I, Leipelt M, Ott C, Zahringer U, Warnecke D, Heinz E (2003) Formation of glucosylceramide and sterol glucoside by a UDP-glucose-dependent glucosylceramide synthase from cotton expressed in Pichia pastoris. FEBS Lett **553:** 365–369

Hobbie L, McGovern M, Hurwitz LR, Pierro A, Liu NY, Bandyopadhyay A, Estelle M (2000) The *axr6* mutants of Arabidopsis thaliana define a gene involved in auxin response and early development. Development **127:** 23–32

Husselstein T, Gachotte D, Desprez T, Bard M, Benveniste P (1996) Transformation of Saccharomyces cerevisiae with a cDNA encoding a sterol C-methyltransferase from Arabidopsis thaliana results in the synthesis of 24-ethyl sterols. FEBS Lett **381:** 87–92

Incardona JP, Eaton S (2000) Cholesterol in signal transduction. Curr Opin Cell Biol **12:** 193–203

Iyer LM, Koonin EV, Aravind L (2001) Adaptations of the helix-grip fold for ligand binding and catalysis in the START domain superfamily. Proteins **43:** 134–144

Jang JC, Fujioka S, Tasaka M, Seto H, Takatsuto S, Ishii A, Aida M, Yoshida S, Sheen J (2000) A critical role of sterols in embryonic patterning and meristem programming revealed by the fackel mutants of Arabidopsis thaliana. Genes Dev **14:** 1485–1497

Kang J, Dengler N (2002) Cell cycling frequency and expression of the homeobox gene ATHB-8 during leaf vein development in Arabidopsis. Planta **216:** 212–219

Kim J, Jung JH, Reyes JL, Kim YS, Kim SY, Chung KS, Kim JA, Lee M, Lee Y, Narry Kim V, et al (2005) MicroRNA-directed cleavage of ATHB15 mRNA regulates vascular development in Arabidopsis inflorescence stems. Plant J **42:** 84–94

Ma Y, Szostkiewicz I, Korte A, Moes D, Yang Y, Christmann A, Grill E (2009) Regulators of PP2C phosphatase activity function as abscisic acid sensors. Science **324:** 1064–1068

Mattsson J, Ckurshumova W, Berleth T (2003) Auxin signaling in Arabidopsis leaf vascular development. Plant Physiol **131:** 1327–1339

McConnell JR, Emery J, Eshed Y, Bao N, Bowman J, Barton MK (2001) Role of PHABULOSA and PHAVOLUTA in determining radial patterning in shoots. Nature **411:** 709–713

Melcher K, Ng LM, Zhou XE, Soon FF, Xu Y, Suino-Powell KM, Park SY, Weiner JJ, Fujii H, Chinnusamy V, et al (2009) A gate-latch-lock mechanism for hormone signalling by abscisic acid receptors. Nature **462:** 602–608

Men S, Boutte Y, Ikeda Y, Li X, Palme K, Stierhof YD, Hartmann MA, Moritz T, Grebe M (2008) Sterol-dependent endocytosis mediates post-cytokinetic acquisition of PIN2 auxin efflux carrier polarity. Nat Cell Biol **10:** 237–244

Miyazono K, Miyakawa T, Sawano Y, Kubota K, Kang HJ, Asano A, Miyauchi Y, Takahashi M, Zhi Y, Fujita Y, et al (2009) Structural basis of abscisic acid signalling. Nature **462:** 609–614

Mravec J, Skupa P, Bailly A, Hoyerova K, Krecek P, Bielach A, Petrasek J, Zhang J, Gaykova V, Stierhof YD, et al (2009) Subcellular homeostasis of phytohormone auxin is mediated by the ER-localized PIN5 transporter. Nature **459:** 1136–1140

Nes WD, McCourt BS, Marshall JA, Ma J, Dennis AL, Lopez M, Li H, He L (1999) Site-directed mutagenesis of the sterol methyl transferase active site from Saccharomyces cerevisiae results in formation of novel 24-ethyl sterols. J Org Chem **64:** 1535–1542

Ohashi Y, Oka A, Rodrigues-Pousada R, Possenti M, Ruberti I, Morelli G, Aoyama T (2003) Modulation of phospholipid signaling by GLABRA2 in root-hair pattern formation. Science **300:** 1427–1430

Ohyama K, Suzuki M, Kikuchi J, Saito K, Muranaka T (2009) Dual biosynthetic pathways to phytosterol via cycloartenol and lanosterol in Arabidopsis. Proc Natl Acad Sci USA **106:** 725–730

Otsuga D, DeGuzman B, Prigge MJ, Drews GN, Clark SE (2001) REVOLUTA regulates meristem initiation at lateral positions. Plant J **25:** 223–236

Paciorek T, Zazimalova E, Ruthardt N, Petrasek J, Stierhof YD, Kleine-Vehn J, Morris DA, Emans N, Jurgens G, Geldner N, et al (2005) Auxin inhibits endocytosis and promotes its own efflux from cells. Nature **435:** 1251–1256

Pan J, Fujioka S, Peng J, Chen J, Li G, Chen R (2009) The E3 ubiquitin ligase SCFTIR1/AFB and membrane sterols play key roles in auxin regulation of endocytosis, recycling, and plasma membrane accumulation of the auxin efflux transporter PIN2 in *Arabidopsis thaliana*. Plant Cell **21:** 568–580

Park SY, Fung P, Nishimura N, Jensen DR, Fujii H, Zhao Y, Lumba S, Santiago J, Rodrigues A, Chow TF, et al (2009) Abscisic acid inhibits type 2C protein phosphatases via the PYR/PYL family of START proteins. Science **324:** 1068–1071

Peng L, Kawagoe Y, Hogan P, Delmer D (2002) Sitosterol-beta-glucoside as primer for cellulose synthesis in plants. Science **295:** 147–150

Ponting CP, Aravind L (1999) START: a lipid-binding domain in StAR, HD-ZIP and signalling proteins. Trends Biochem Sci **24:** 130–132

Prigge MJ, Otsuga D, Alonso JM, Ecker JR, Drews GN, Clark SE (2005) Class III homeodomain-leucine zipper gene family members have overlapping, antagonistic, and distinct roles in *Arabidopsis* development. Plant Cell **17:** 61–76

Przemeck GK, Mattsson J, Hardtke CS, Sung ZR, Berleth T (1996) Studies on the role of the Arabidopsis gene MONOPTEROS in vascular development and plant cell axialization. Planta **200:** 229–237

Robert HS, Friml J (2009) Auxin and other signals on the move in plants. Nat Chem Biol **5:** 325–332

Santiago J, Dupeux F, Round A, Antoni R, Park SY, Jamin M, Cutler SR, Rodriguez PL, Marquez JA (2009) The abscisic acid receptor PYR1 in complex with abscisic acid. Nature **462:** 665–668

Schaeffer A, Bronner R, Benveniste P, Schaller H (2001) The ratio of campesterol to sitosterol that modulates growth in Arabidopsis is controlled by STEROL METHYLTRANSFERASE 2;1. Plant J **25:** 605–615

Schaller H (2004) New aspects of sterol biosynthesis in growth and development of higher plants. Plant Physiol Biochem **42:** 465–476

Schaller H, Bouvier-Nave P, Benveniste P (1998) Overexpression of an Arabidopsis cDNA encoding a sterol-C24(1)-methyltransferase in tobacco modifies the ratio of 24-methyl cholesterol to sitosterol and is associated with growth reduction. Plant Physiol **118:** 461–469

Schrick K, Fujioka S, Takatsuto S, Stierhof YD, Stransky H, Yoshida S, Jurgens G (2004a) A link between sterol biosynthesis, the cell wall, and cellulose in Arabidopsis. Plant J **38:** 227–243

Schrick K, Mayer U, Horrichs A, Kuhnt C, Bellini C, Dangl J, Schmidt J, Jurgens G (2000) FACKEL is a sterol C-14 reductase required for organized cell division and expansion in Arabidopsis embryogenesis. Genes Dev **14:** 1471–1484

Schrick K, Mayer U, Martin G, Bellini C, Kuhnt C, Schmidt J, Jurgens G (2002) Interactions between sterol biosynthesis genes in embryonic development of Arabidopsis. Plant J **31:** 61–73

Schrick K, Nguyen D, Karlowski WM, Mayer KF (2004b) START lipid/sterol-binding domains are amplified in plants and are predominantly associated with homeodomain transcription factors. Genome Biol **5:** R41

Sekimata K, Kimura T, Kaneko I, Nakano T, Yoneyama K, Takeuchi Y, Yoshida S, Asami T (2001) A specific brassinosteroid biosynthesis inhibitor, Brz2001: evaluation of its effects on Arabidopsis, cress, tobacco, and rice. Planta **213:** 716–721

Sheard LB, Zheng N (2009) Plant biology: signal advance for abscisic acid. Nature **462:** 575–576

Sieburth LE (1999) Auxin is required for leaf vein pattern in Arabidopsis. Plant Physiol **121:** 1179–1190

Simons K, Ikonen E (1997) Functional rafts in cell membranes. Nature **387:** 569–572

Souter M, Topping J, Pullen M, Friml J, Palme K, Hackett R, Grierson D, Lindsey K (2002) *hydra* mutants of *Arabidopsis* are defective in sterol profiles and auxin and ethylene signaling. Plant Cell **14:** 1017–1031

Souter MA, Pullen ML, Topping JF, Zhang X, Lindsey K (2004) Rescue of defective auxin-mediated gene expression and root meristem function by inhibition of ethylene signalling in sterol biosynthesis mutants of Arabidopsis. Planta **219:** 773–783

Szostkiewicz I, Richter K, Kepka M, Demmel S, Ma Y, Korte A, Assaad FF, Christmann A, Grill E (2010) Closely related receptor complexes differ in their ABA selectivity and sensitivity. Plant J **61:** 25–35

Ulmasov T, Murfett J, Hagen G, Guilfoyle TJ (1997) Aux/IAA proteins repress expression of reporter genes containing natural and highly active synthetic auxin response elements. Plant Cell **9:** 1963–1971

Willemsen V, Friml J, Grebe M, van den Toorn A, Palme K, Scheres B (2003) Cell polarity and PIN protein positioning in *Arabidopsis* require STEROL METHYLTRANSFERASE1 function. Plant Cell **15:** 612–625

Yin P, Fan H, Hao Q, Yuan X, Wu D, Pang Y, Yan C, Li W, Wang J, Yan N (2009) Structural insights into the mechanism of abscisic acid signaling by PYL proteins. Nat Struct Mol Biol **16:** 1230–1236